Effect of Kármán Vortex Shedding on Airfoil Stall Flutter

L. E. Ericsson*
Lockheed Missiles & Space Company, Inc., Sunnyvale, California

An analysis of available experimental stall flutter data shows that, whereas the attitude-Mach number (α-M_∞) stall flutter boundary is determined mainly by compressibility effects, the reduced frequency boundary is not. It is instead generated by an aerodynamically damping interaction with Kármán vortex shedding at reduced frequencies $\omega c/U_\infty > 2$.

Nomenclature

a = speed of sound
c = chord length
f = frequency, $= T^{-1}$
f_0 = natural structural frequency
f_v = frequency of Kármán vortex shedding
f_{v0} = f_v for stationary conditions
h = cross-sectional height
k = reduced frequency parameter, $= \bar{\omega}/2$
el = sectional lift, coefficient $c_\ell = \ell/(\rho_\infty U_\infty{}^2/2)c$
M = Mach number, $= U/a$
m = sectional pitching moment, coefficient $c_m = m/(\rho_\infty U_\infty{}^2/2)c$
Re = Reynolds number, usually $= U_\infty c/\nu\infty$
r_N = nose radius
S = Strouhal number, $= fh/U_\infty$
S^* = modified Strouhal number, $= fc/U_\infty$
T = oscillation period
t = time
U = velocity
$\bar{V}$ = reduced velocity, $= S^{-1}$
z = translatory coordinate
α = angle of attack
Δ = increment or amplitude
ν = kinematic viscosity of air
ρ = air density
ρ_N = dimensionless nose radius, $= r_N/c$
ω = angular oscillation frequency, $= 2\pi f$
$\bar{\omega}$ = reduced frequency, $= \omega c/U_\infty$

Subscripts

cr = critical ($S = S_{v0}$)
max = maximum
N = nose
SB = stability boundary
1,2 = numbering subscript
∞ = undisturbed flow

Differential Symbol

$\dot{\alpha}$ = $\partial\alpha/\partial t$

Introduction

In the early 1970's, the problem of stall flutter, which always has been of great concern to helicopter and compressor manufacturers, became of concern also to the aerospace industry. The earliest Space Shuttle configurations considered had wings that would be exposed to stall flutter during the transition maneuver from the very high entry attitude to the substall angle of attack necessary for the subsonic cruise.[1] Tests verified that there was a stall flutter problem.[2] (See Fig. 1) The attitude-Mach number (α-M_∞) flutter boundary, shown in more detail in Fig. 2, could be predicted.[3] However, although it was surmised in Ref. 3 that the experimentally observed high-frequency flutter boundary, $\bar{\omega} \approx 2$ in Fig. 1, was probably the result of an interaction between Kármán vortex shedding and the torsional oscillation of the wing, the detailed fluid dynamic process through which it would occur was not fully understood at the time. Recent analysis of the aeroelastic stability of the cable trays on the current Space Shuttle launch vehicle[4,5] has provided the fluid dynamics insight needed to describe the interaction between Kármán vortex shedding and airfoil oscillation.

Compressibility effects are important in regard to airfoil stall characteristics, as the peak velocity on the airfoil at stall is several times higher than at zero angle of attack[3] and can exceed sonic speed at freestream Mach numbers below $M_\infty = 0.3$ (Fig. 3). The experimental results[6] are in good agreement with predictions.[3] This compressibility effect severely restricts the maximum lift that can be obtained in wind-tunnel tests[7] or full-scale flight[8] (Fig. 4). It completely dominates over the effect of varying Reynolds numbers in the test and is responsible for the sharp decrease of the stall angle with increasing Mach number in the stall flutter boundary (Fig. 2). It has been suggested[2] that the high-frequency cutoff of stall flutter for $\bar{\omega} > 2$ could also be caused by Mach number effects. The present analysis shows this not to be the case. It is, instead, the Kármán vortex shedding that is responsible for the high-frequency cutoff.

Discussion

For rectangular cross sections with $c/h < 2.5$, negative lift slopes are measured[9] (Fig. 5), resulting in an instability in bending or plunging oscillations (often called "galloping" instability[10]). The maximum limit cycle amplitude of such oscillations can be predicted analytically.[10,11] The experimentally observed amplitude[12] falls, as expected, below this prediction (Fig. 6). However, only for $\bar{V} > \bar{V}_{cr} \approx 11$ is the behavior the expected one. For oscillations above the Strouhal frequency,† i.e., for $\bar{V} < \bar{V}_{cr}$, where $\bar{V}_{cr} = S_{v0}{}^{-1}$, the response amplitude goes to zero. A similar behavior has been observed for a circular cylinder.[13,14] It is shown in Ref. 12 how the damping influence at $\bar{V} < \bar{V}_{cr}$ is caused by the interaction between body motion and Kármán vortex shedding. Figure 7 shows the Kármán vortex

Presented as Paper 86-1789 at the AIAA 4th Applied Aerodynamics Conference, San Diego, CA, June 9-11, 1986; received June 7, 1986; revision received April 23, 1987. Copyright ©1987 by L. Ericsson. Published by the American Institute of Aeronautics and Astronautics, Inc., with permission.

*Senior Consulting Engineer. Fellow AIAA

†The amplitude response around $\bar{V} = 5$ is caused by the superharmonic response discussed in Ref. 12.

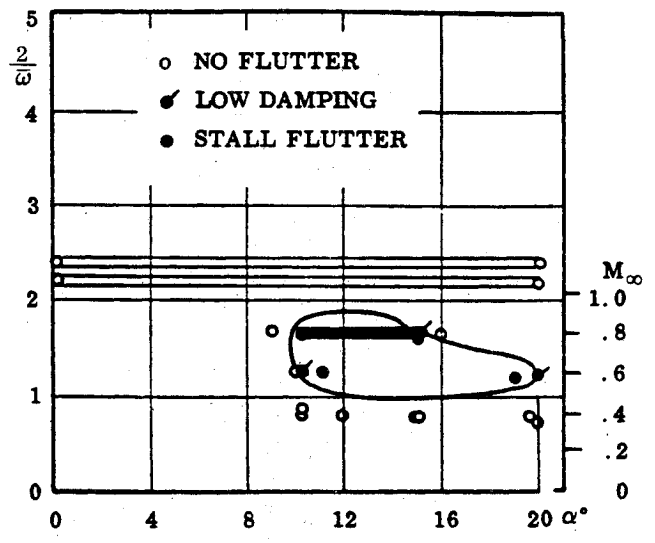

Fig. 1 Stall flutter boundaries of a NACA 0012 airfoil (from Ref. 2).

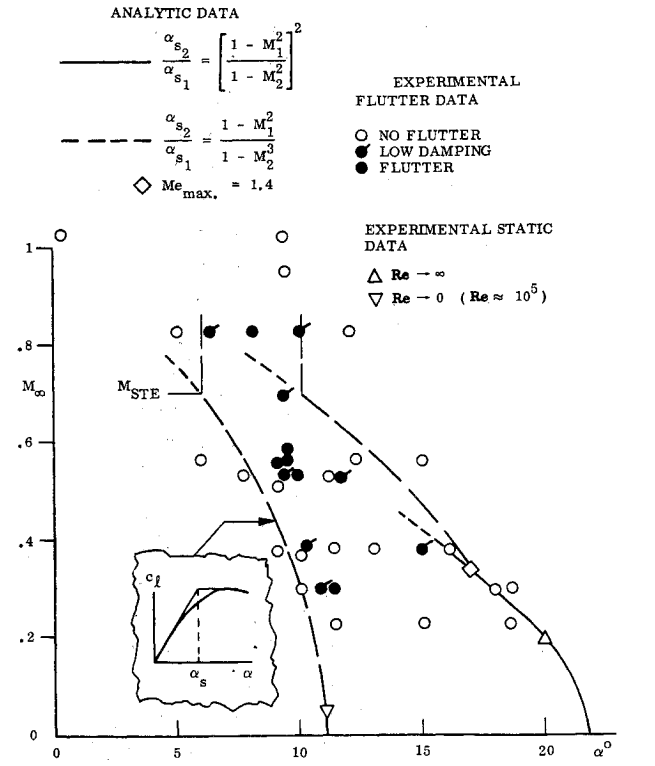

Fig. 2 Predicted and measured α-M_∞ stall flutter boundaries (from Ref. 3).

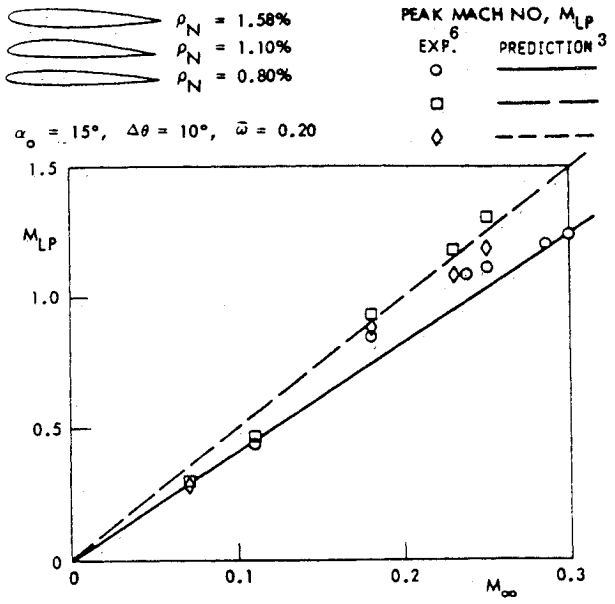

Fig. 3 Peak Mach number on stalling airfoils.

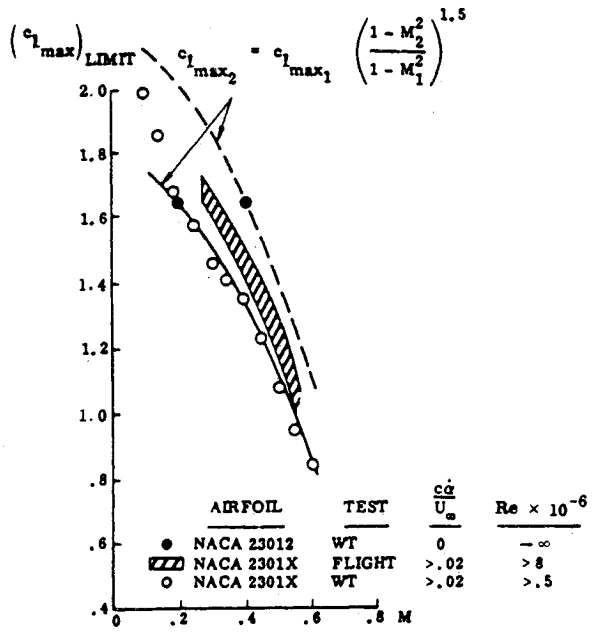

Fig. 4 Maximum lift as a function of Mach number for a NACA 230XX airfoil (from Ref. 3).

shedding frequency measured on rectangular cross sections,[15-17] as well as the vortex structures observed through flow visualization.[17,18] When the flow separation from the leading edge reattaches before the trailing edge, for $c/h > 2.5$, the resulting reduction of the wake width causes an increase of the Strouhal frequency, referenced to the cross-sectional height, $S_{v0} = f_{v0}h/U_\infty$. For plunging oscillations, the main effect is that of the so-called "moving wall" between flow stagnation and separation points.[12,19] The predicted[12] and experimental[16,20] stability boundaries lie close to V_{cr} (Fig. 8).

The pitching moment around midchord is statically stabilizing at $\alpha = 0$ even for $c/h = 4$ (Fig. 5). Due to the effect of time lag, the dynamic effect is destabilizing.[12,21] Thus, torsional oscillations around midchord show the same type of amplitude divergence as plunging oscillations[20] (Fig. 9). In the case of torsional oscillations, the vortex-induced loads on the rectangular cross section become important and the predicted[12] and experimental[9,16,20] stability boundaries no longer coincide with V_{cr} (Fig. 10). A typical example of torsional, stall flutter-type instability is shown in Fig. 11.

Recent experimental results for a NACA 0015 airfoil, describing a pitch-up motion around the quarter chord at a constant pitch rate, show an oscillatory lift behavior after stall that appears to be of the constant-frequency type associated with Kármán vortex shedding[22] (Fig 12). Similar behavior was observed by Ham and Garelick[23] (Fig. 13), although they did

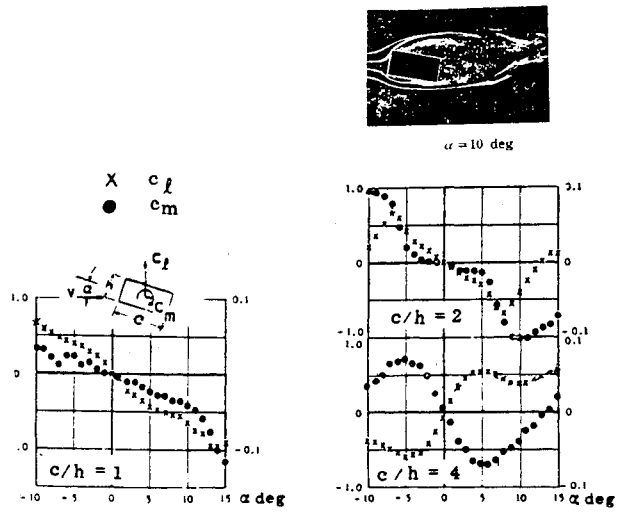

Fig. 5 Aerodynamic low-speed characteristics of a $c/h=2$ rectangular prism (from Ref. 9).

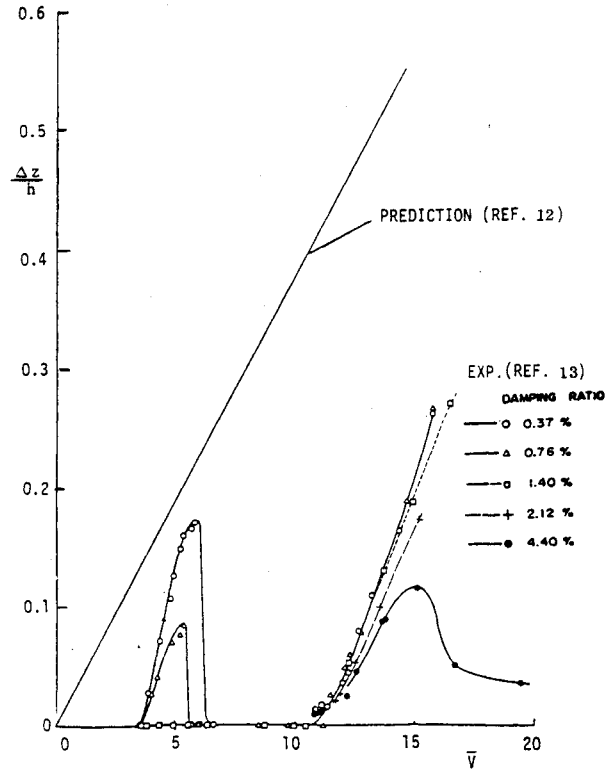

Fig. 6 Predicted and measured galloping response of a $c/h=2$ rectangular cross section.

not have enough data for a full evaluation of the poststall lift behavior. The initial first half-amplitude of the lift oscillation could, however, be predicted.[24] It is determined by the (initial) conditions at stall, similar to the shock oscillation associated with shock-induced flow separation.[25] This explains the repeatability of the lift oscillations in Fig. 12.

That is, the initiation as well as the amplitude of the ensuing oscillation is determined by the dynamic conditions leading to airfoil stall and the associated shedding of a leading-edge vortex. However, the frequency of the oscillation is determined by the width of the airfoil wake,[19] independent of any nonoscillatory motion of the wake-generating body. The effect of the present α ramp is similar to the effect of steady rotation on the Kármán vortex shedding from a circular cylinder,[26] i.e., there is no effect on the frequency of the vortex shedding. There is, however, an effect on the quasisteady aerodynamic characteristics on which the vortex-induced effects are superimposed. Thus, comparing Figs. 12 and 13 with the static airfoil results[27] in Fig. 14, one can see how the α ramp appears to have a lift-generating effect similar to the Magnus lift-generating effect of a rotating circular cylinder.[28] This is in agreement with the observed universality of so-called moving-wall effects.[29] Thus, regardless of how the moving-wall effect is generated, it cannot affect the frequency of the vortex shedding unless the moving-wall effect is itself oscillatory in nature, as in the case of airfoil oscillations in pitch, for example. In that case, the oscillation frequency has to be in a range in which the so-called lock-on of the Kármán vortex shedding can occur.[19]

Analysis

The pitch rate for the results in Fig. 12 was $\dot{\alpha}c/U_\infty = 0.0524$. The peak-to-peak α spread is $\Delta\alpha \approx 10$ deg $= 0.174$. With $T = f^{-1} = \Delta\alpha/\dot{\alpha}$, one obtains $fc/U_\infty \approx 0.0524/0.174 = 0.30$, giving $\bar{\omega} = 2\pi fc/U_\infty = 1.9$, which is in good agreement with the cutoff frequency for stall flutter in Fig. 1. (That Kármán vortex shedding occurs on a stalling airfoil has been observed experimentally.[30])

For $\alpha \approx 30$ deg in Fig. 12, $h = \sin\alpha = c/2$ and $fh/U_\infty \approx 0.15$. This is in good agreement with the results in Fig. 7 for rectangular cross sections with $c/h \geq 3$.

The results in Fig. 7 show that the width of the vortex wake increases with increasing chord length. As the Strouhal number based on wake width remains constant[19] when it is referenced to the cross-sectional height, $S_{v0} = f_{v0}\, h/U_\infty$, it decreases with increasing c/h. A similar trend, probably even more pronounced, will be present for the airfoil. When the angle of attack is increased beyond the stall angle, the wake width remains more or less constant up to very large angles of attack. Consequently, the wake width for the α region $10 < \alpha < 20$ deg in Fig. 1 is probably the same as for $\alpha = 30$ deg, giving $\bar{\omega} = 1.9$— in good agreement with the observed high-frequency limit for stall flutter.[2] (See Fig. 1.)

Experimental results for a square cross-sectional cylinder[31] tend to support this speculation. The spectrum also contains the sharp spike associated with Kármán vortex shedding at $\alpha = 13.5$ deg, where the windward side flow is attached (Fig. 15). The only difference is that the shedding frequency has increased at $\alpha = 13.5$ deg compared to $\alpha = 0$. This has also been observed by others,[32-34] in which case the frequency change was of a more continuous character (Fig. 16). That is, the Kármán vortex wake is very similar for the two cases of attached or separated windward side flow.

On an airfoil, at $\alpha = 0$, the flow is attached over most of the surface. As the angle of attack is increased, the wake size increases, causing a rapid drop of the Strouhal number of the Kármán vortex shedding until at high angles of attack the wake size and hence the frequency remains constant[35] (Fig. 17). The data in Fig. 17 for $Re = 0.05 \times 10^5$ give $\bar{\omega} \approx 2.75$ for $\alpha < -15$ or > 20 deg. It is a fact that the wake size decreases with increasing Reynolds number, which in turn decreases the Strouhal number of the Kármán vortex shedding.[19] This has been demonstrated for a square cross section[31] (Fig. 18). Thus, the value $\bar{\omega} \approx 2.75$ for $Re = 0.05 \times 10^5$ in Fig. 17 is in satisfactory agreement with the value $\bar{\omega}_{SB} \approx 2$ for $Re \approx 10^5$ in Fig. 1. On expects the Reynolds number effect to be much larger for a round-nosed airfoil than for the sharp-edged cross section in Fig. 18.

An alternate explanation for the high-frequency limit for stall flutter has been suggested.[2] At a pitch frequency $\omega c/a = 1$, i.e., $\bar{\omega} = M_\infty^{-1}$, the leading and trailing edges move at sonic velocity relative to each other. One can visualize how, at higher pitching frequencies, shocks will cut off the communication between the wake and airfoil, as has been observed for slender bodies.[36]

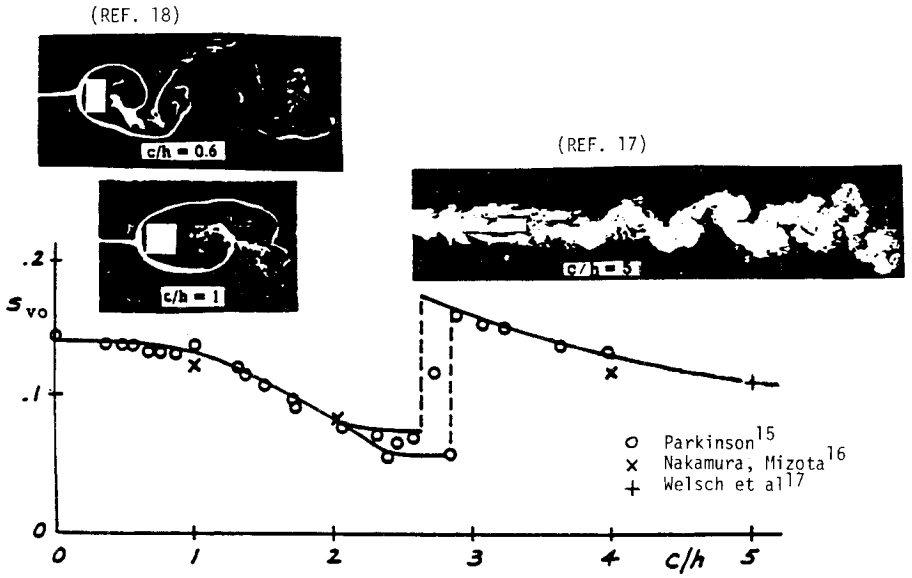

Fig. 7 Strouhal number of Kármán vortex shedding from rectangular cross sections.

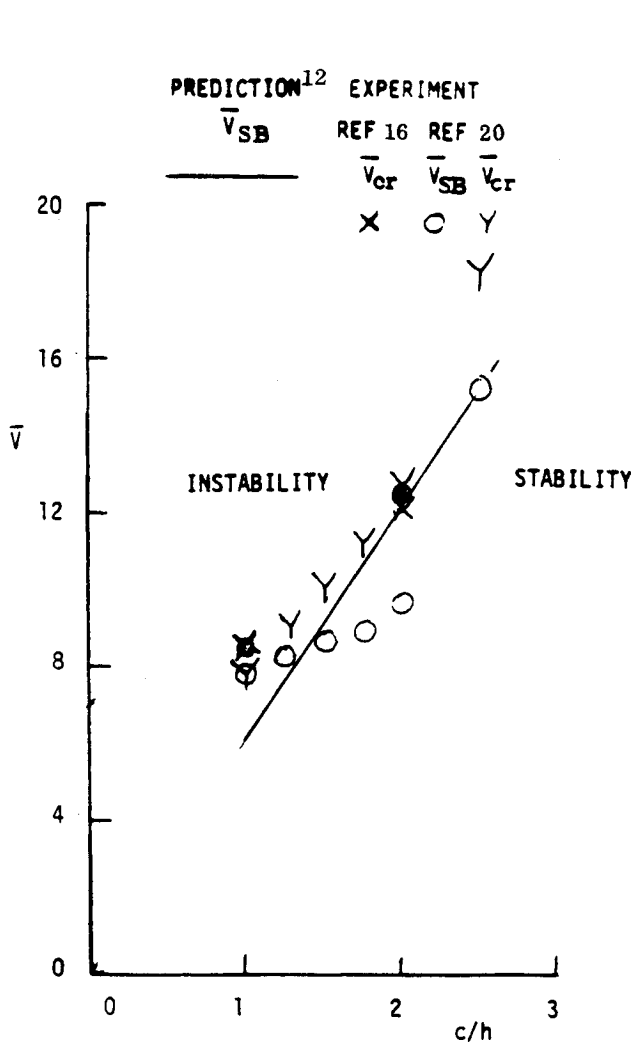

Fig. 8 Predicted and measured stability boundaries of galloping rectangular cylinders.

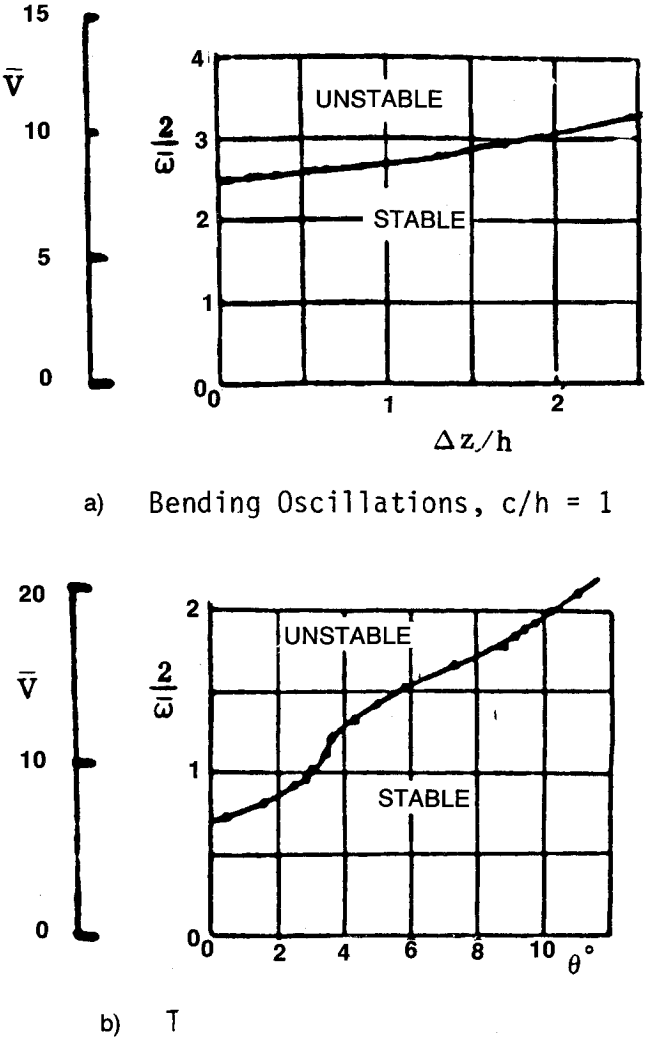

Fig. 9 Amplitude response of rectangular cylinders in plunging and torsional oscillations (from Ref. 20) a) bending oscillations, $c/h = 1$; b) torsional oscillations, $c/h = 3$.

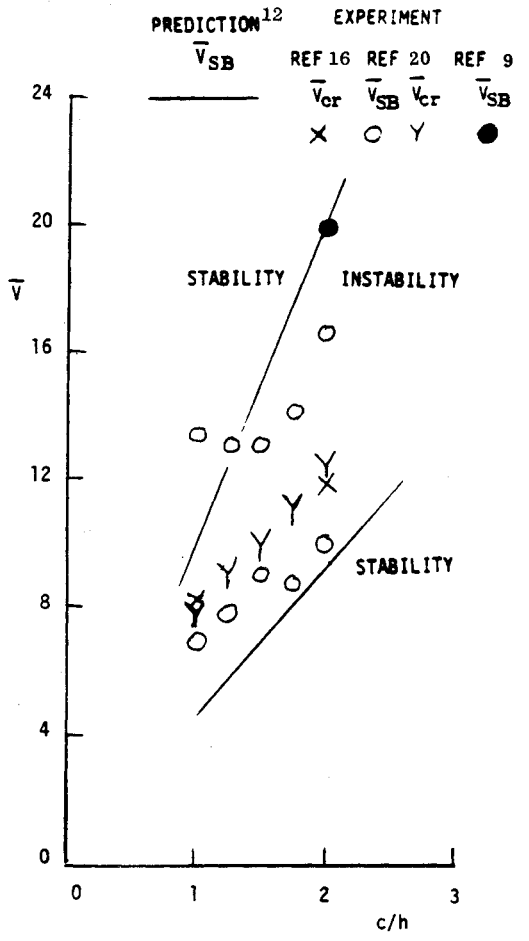

Fig. 10 Predicted and measured stability boundaries for torsional oscillations (stall flutter) of rectangular cross sections.

However, the results in Fig. 9 and associated analysis[12] clearly show that stall flutter and galloping are the same type of self-excited oscillations, both resulting in limit cycle amplitude oscillations unless the frequency is such that the damping effect of Kármán vortex shedding can be realized. Thus, one would expect self-excited wing bending or plunging oscillations to have a high-frequency cutoff similar to the torsional oscillations in Fig. 1, in which case there is no relative velocity between the leading and trailing edges. That is, available experimental results strongly suggest that the high-frequency limit of stall flutter is generated by the damping effect of Kármán vortex shedding at frequencies above $\bar{\omega} \approx 2$.

Conclusions

A review and analysis of existing experimental stall flutter results has led to the following conclusions:

1) The high-frequency stall flutter boundary at $\bar{\omega} \approx 2$ or $k \approx 1$ is a result of the damping interaction of Kármán vortex shedding at higher frequencies.

2) The stall flutter behavior is of the same character for torsional and bending oscillations, indicating that the elimination of stall flutter at $\bar{\omega} > 2$ is not due to supersonic relative translatory velocities between the leading and trailing edges, as this can occur only for torsional oscillations, not for bending or plunging oscillations.

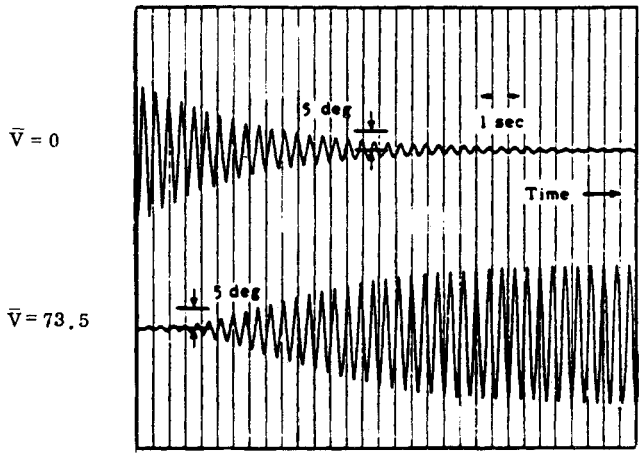

Fig. 11 Torsional amplitude response of a $c/h = 5$ rectangular cylinder (from Ref. 9).

References

[1]Runyan, H.L. and Reed, W. H., "Dynamics and Aeroelasticity—An Appraisal," *Astronautics & Aeronautics,* Vol. 9, Feb. 1971, pp. 48–57.

[2]Goetz, R. C., "Exploratory Study of Buffet and Stall Flutter of Space Vehicle Wing Concepts," NASA LWP-872, May 1970.

[3]Ericsson, L. E. and Reding, J. P., "Stall-Flutter Analysis," *Journal of Aircraft,* Vol. 10, Jan. 1973, pp. 5–13.

[4]Ericsson, L. E. and Reding, J. P., "Aeroelastic Stability of Space Shuttle Protuberances," *Journal Spacecraft and Rockets,* Vol. 19, July–Aug. 1982, pp. 307–313.

[5]Ericsson, L. E. and Reding, J. P., "Aeroelastic Characteristics of the Space Shuttle External Tank Cable Trays," *Journal of Spacecraft and Rockets,* Vol. 22, May–June 1985, pp. 289–296.

[6]McCroskey, W. J., McAllister, K. W., Carr, L. W., and Pucci, S. L., "An Experimental Study of Dynamic Stall on Advanced Airfoil Sections, Vol. 1: Summary of the Experiment," NASA TM-84245, July 1982.

[7]Harper, P. W. and Flanigan, R. E., "The Effect of Rate of Change of Angle of Attack on the Maximum Lift of a Small Model," NACA TN-2061, 1949.

[8]Harper, P. W. and Flanigan, R. E., "Investigation of the Variation of Maximum Lift for a Pitching Airplane Model and Comparison with Flight Results," NACA TN-1734, 1937.

[9]Nakamura, Y. and Mizota, T., "Torsional Flutter of Rectangular Prisms," *Journal of the Engineering Mechanics Division, ASCE,* Vol. 101, No. EM2, April 1975, pp. 125–143.

[10]Ericsson, L. E., "Limit Amplitude of Galloping Cables," *AIAA Journal,* Vol. 22, April 1984, pp. 493–497.

[11]Ericsson, L. E., "Hydroelastic Effects of Separated Flows," *AIAA Journal,* Vol. 21, March 1983, pp. 452–458.

[12]Ericsson, L. E., "Kármán Vortex Shedding, Friend or Foe of the Structural Dynamicist?" *Journal of Aircraft,* Vol. 23, Aug. 1986, pp. 621–628.

[13]Novak, M., "Galloping and Vortex Induced, Oscillations of Structures," *Proceedings of 3rd Conference on Wind Effects on Buildings and Structures,* Tokyo, Sept. 1971, pp. 799–809.

[14]Ferguson, M. and Parkinson, G. V., "Surface and Wake Phenomena of the Vortex-Excited Oscillation of a Circular Cylinder," *Transactions of ASME, Journal of Engineering for Industry,* Vol. 89, No. 3, Nov. 1967, pp. 831–838.

[15]Parkinson, G. V., "Aeroelastic Galloping in One Degree of Freedom," *Proceedings of 1963 Conference on Wind Effects on Buildings and Structures,* Vol. II, HMSO, London, 1965, pp. 582–609.

[16]Nakamura, Y. and Mizota, T., "Unsteady Lifts and Wakes of Oscillating Rectangular Prisms," *Journal of the Engineering Mechanics Division, ASCE,* Vol. 101, No. EM6, Dec. 1975, pp. 855–871.

[17]Welsh, M. C., Parker, R., and Stoneware, S.A.T., "Effect of Induced Sound on the Flow Around a Rectangular Body in a Wind Tunnel," *Proceedings of 7th Australasian Hydraulics and Fluid Mechanics Conference,* Brisbane, Aug. 1980, pp. 275–278.

[18]Bearman, P. W. and Trueman, D. M., "An Investigation of the Flow Around Rectangular Cylinders," *Aeronautical Quarterly,* Aug. 1972, pp. 229–237.

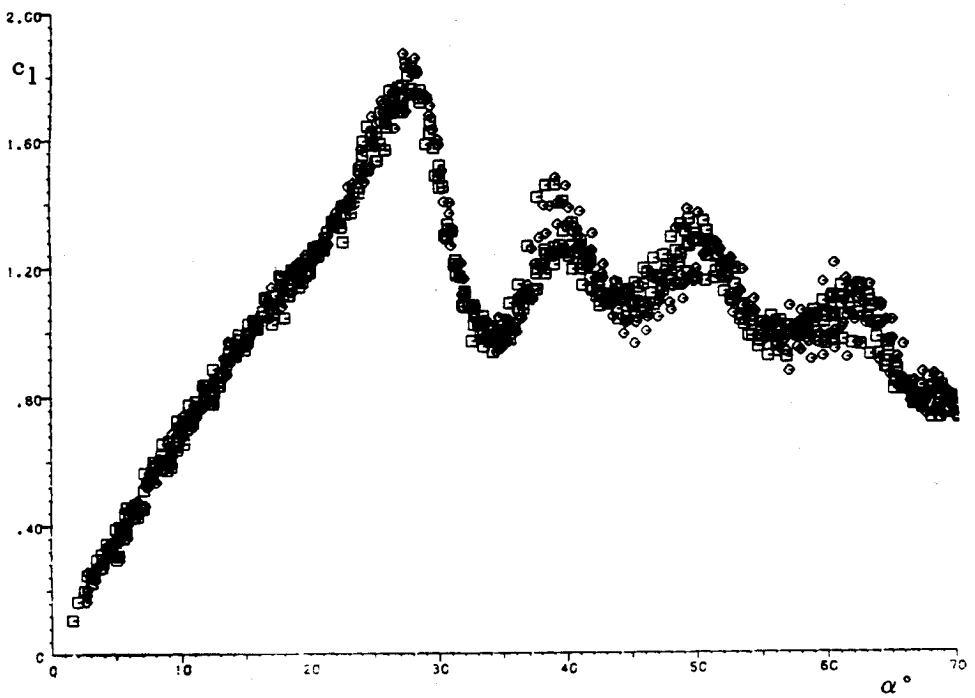

Fig. 12 Low-speed alpha-ramp response of a NACA 0015 airfoil (from Ref. 22).

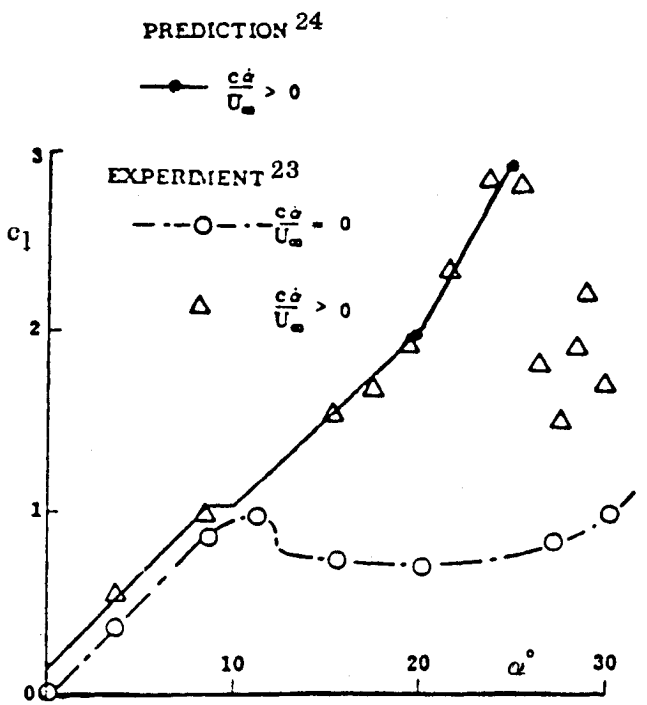

Fig. 13 Predicted and measured alpha-ramp response of a NACA 0012 airfoil.

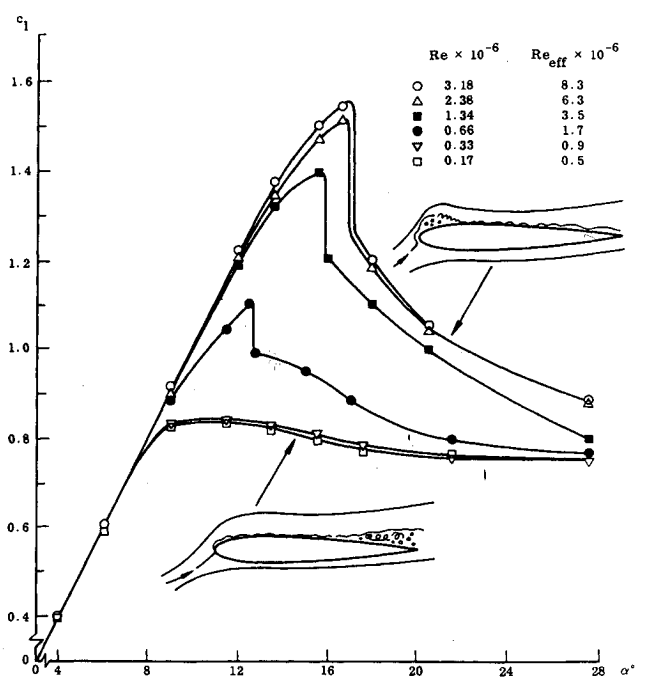

Fig. 14 Effect of Reynolds number on the lift characteristics of the NACA 0012 airfoil (from Ref. 27).

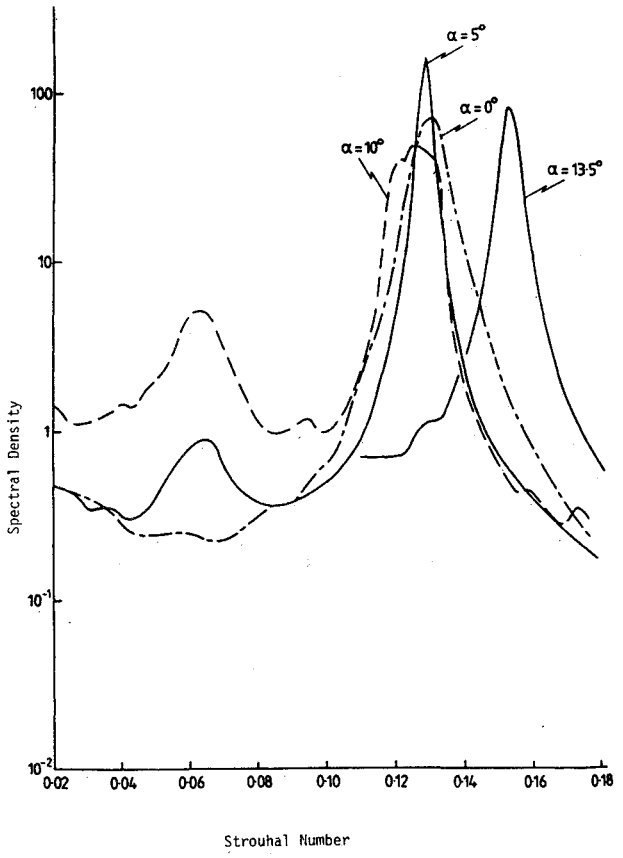

Fig. 15 Effect of angle of attack on the fluctuating pressure on a square cross section (from Ref. 31).

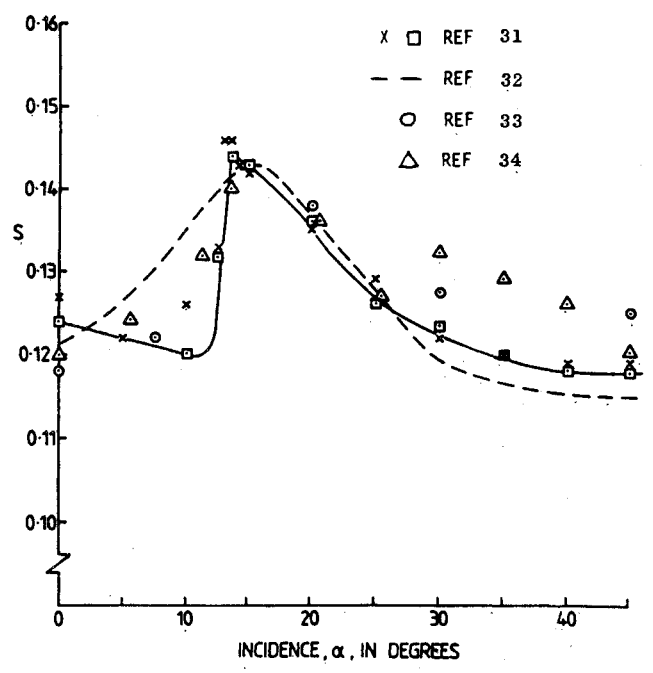

Fig. 16 Effect of angle of attack on the Strouhal number of Kármán vortex shedding from a square cylinder.

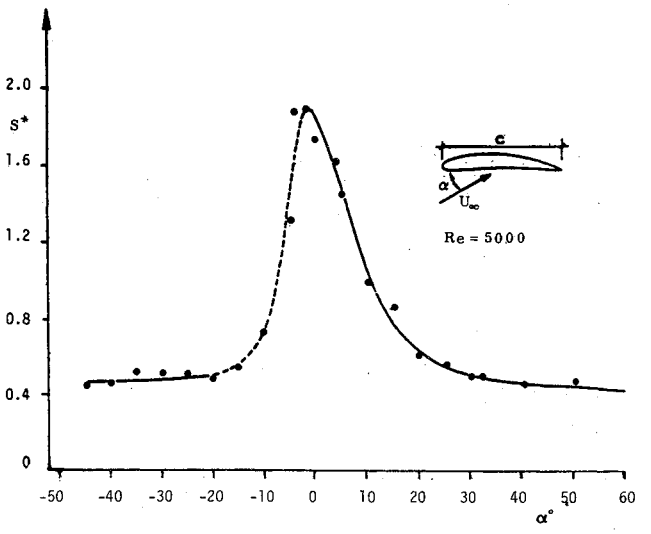

Fig. 17 Effect of angle of attack on the chord-based Strouhal frequency S^* of a cambered airfoil (from Ref. 35).

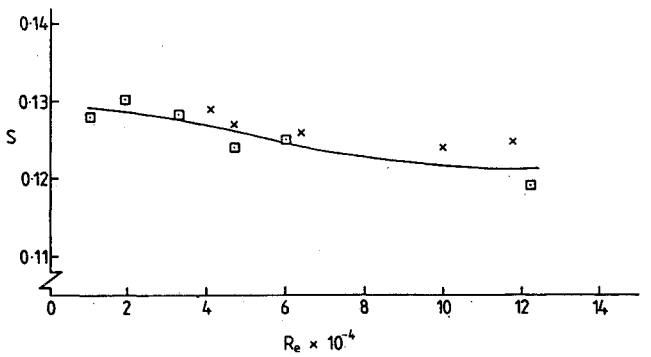

Fig. 18 Variation of Strouhal number with Reynolds number for a square cross section at $\alpha = 0$ (from Ref. 31).

[19]Ericsson, L. E., "Kármán Vortex Shedding and the Effect of Body Motion," *AIAA Journal,* Vol. 18, Aug. 1980, pp. 935-944.

[20]Otsuki, Y., Washizu, K., Tomizawa, H., Ohya, A., and Fujii, K., "Experiments on the Aeroelastic Stability of Prismatic Bars with Rectangular Sections," *Proceedings of 3rd Conference on Wind Effects on Buildings and Structures,* Tokyo, Sept. 1971, pp. 891-898.

[21]Ericsson, L. E. and Reding, J. P., "Dynamic Stall Analysis in Light of Recent Numerical and Experimental Results," *Journal of Aircraft,* Vol. 13, April 1976, pp. 248-255.

[22]Jumper, E. J., Dimmick, R. L., and Schreck, S. J., "Lift Curve Characteristics for an Airfoil Pitching at Constant Rate," AIAA Paper 86-0117, Jan. 1986.

[23]Ham, N. D. and Garelick, M. S., "Dynamic Stall Considerations in Helicopter Rotors," *American Helicopter Society Journal,* Vol. 13, April 1968, pp. 44-55.

[24]Ericsson, L. E. and Reding, J. P., "Dynamic Stall at High Frequency and Large Amplitude," *Journal of Aircraft,* Vol. 17, March 1980, pp. 136-142.

[25]Ericsson, L. E., "Dynamic Effects of Shock-Induced Flow Separation, *Journal of Aircraft,* Vol. 12, Feb. 1975, pp. 86-92.

[26]Diaz, F., Gavalda, J., Kawall, J. G., Keller, J. F., and Giralt, F., "Vortex Shedding from a Spinning Cylinder," *The Physics of Fluids,* Vol. 26, Dec. 1983, pp. 3454-3460.

[27]Jacobs, E. N. and Sherman, A., "Airfoil Section Characteristics as Affected by Variations in the Reynolds Number," NACA TR 586, 1937.

[28]Swanson, W. M., "The Magnus Effect: A Summary of Investigations to Date," *Transactions of ASME, Journal of Basic Engineering,* Vol. 83, Sept. 1961, pp. 461-470.

[29]Ericsson, L. E., "Dynamic Omnipresence of Moving Wall Effects," AIAA Paper 87-0241, Jan. 1987.
[30]Scruggs, R. M., "An Investigation of Near Wake Effects in Airfoil Dynamic Stall," School of Aerospace Engineering, Georgia Institute of Technology, Atlanta, Report 71-1, March 1971.
[31]Obasaju, E. D., "An Investigation of the Effects of Incidence on the Flow Around a Square Section Cylinder," *Aeronautical Quarterly,* Nov. 1983, pp 243–259.
[32]Lee, B. E., "The Effect of Turbulence on the Surface Pressure Field on a Square Prism," *Journal of Fluid Mechanics,* Vol. 69, 1975, pp. 263–282.
[33]Vickery, B.J., "Fluctuating Lift and Drag on a Long Clyinder of Square Cross-Section in Smooth and in Turbulent Stream," *Journal of Fluid Mechanics,* Vol. 25, 1966, pp. 481–494.
[34]Pocha, J. J., "On Unsteady Flow Past Cylinders of Square Cross-Section," Ph.D. Thesis, Dept. of Aeronautics, Queen Mary College, London University, London, 1971.
[35]Cenedese, A., Cerri, G., and Ianetta, S., "LDV Analysis of Wakes Behind Circular Cylinders and Airfoils, *Meccanica,* Dec. 1981, pp. 220–231.
[36]Ericsson, L. E. and Reding, J. P., "Aerodynamic Effects of Bulbous Bases," NASA CR-1339, Aug. 1969.

From the AIAA Progress in Astronautics and Aeronautics Series . . .

TRANSONIC AERODYNAMICS—v. 81

Edited by David Nixon, Nielsen Engineering & Research, Inc.

Forty years ago in the early 1940s the advent of high-performance military aircraft that could reach transonic speeds in a dive led to a concentration of research effort, experimental and theoretical, in transonic flow. For a variety of reasons, fundamental progress was slow until the availability of large computers in the late 1960s initiated the present resurgence of interest in the topic. Since that time, prediction methods have developed rapidly and, together with the impetus given by the fuel shortage and the high cost of fuel to the evolution of energy-efficient aircraft, have led to major advances in the understanding of the physical nature of transonic flow. In spite of this growth in knowledge, no book has appeared that treats the advances of the past decade, even in the limited field of steady-state flows. A major feature of the present book is the balance in presentation between theory and numerical analyses on the one hand and the case studies of application to practical aerodynamic design problems in the aviation industry on the other.

Published in 1982, 669 pp., 6×9, illus., $45.00 Mem., $75.00 List

TO ORDER WRITE: Publications Dept., AIAA, 370 L'Enfant Promenade S.W., Washington, D.C. 20024-2518